Analysis of Multicore Fibre Transmission with Space Coding Scheme

Makoto Tsubokawa
Waseda University, 2-7 Hibikino, Wakamatsu, Kitakyusyu, 808-0135, Japan

Keywords: Multicore Fibre, Space Division Multiplexing, Optical Code Division Multiplexing, Optical Transmission System.

Abstract: We analysed the space coding scheme applied to the space division multiplexing transmission in two types of multicore fibres with different intercore crosstalk. Rather than the usual optical multiple-input and multiple-output processing, simple space coding based on optical code division multiplexing was used to achieve separate detection of the desired signals. The signal to interference-and-noise ratio has a positive value when the relative phase drift between the optical signals in different cores is suppressed to values typically less than ~π/10. Although a complete solution of the phase drift control problem was not achieved, this scheme suggests that real-time MCF transmissions are possible.

1 INTRODUCTION

Space division multiplexing (SDM) with multicore fibres (MCFs) has received considerable attention to expand transmission capacity further (Sakaguchi et al., 2013; Hayashi et al., 2011; Xia et al., 2012). However, owing to complicated system architecture, several difficulties still remain; in particular, the computational complexity of optical multi-input multi-output (MIMO) processing is not avoidable to mitigate the signal degradation because of the intercore crosstalk (CT) (Ryf et al., 2011; Winzer et al., 2011). Moreover, SDM with a multimode fibre has been intensively studied in recent years, and optical MIMO processing was found to be essential for compensating complex intermode couplings (Shah et al., 2005; Sakamoto et al., 2015; Arik et al., 2013). Although low CT is preferable, MCF design and fabrication have been hindered by the requirement for a trade-off between the number of cores and CT severity. Code division multiplexing (CDM) may be an effective scheme for reduction of the CT-generated noise. In optical transmissions other than free-space optics, optical CDM in time and/or wavelength domains has been commonly used (Mendez et al., 2003; Hernandez et al., 2005; Kitayama et al., 2006), while space coding has been rarely reported because there are very few applicable transmission media having lesser multipath fading. However, in an MCF, the variation of the multipath fading must be homogenised because of the similar cores and their arrangement in an MCF.

In this study, we show for the first time the possibility of application of simple optical space coding to MCF transmission without optical MIMO processing. The space coding is expected to reduce the CT-generated noise caused in a MCF with large CT. Our proposed scheme is applied to two types of MCFs with strong and weak intercore couplings; moreover, the separate detection of the desired signal buried in the noise is theoretically evaluated.

2 SPACE CODING SCHEME

A schematic of the SDM transmission line with a multi-core single mode optical fibre is shown in Fig. 1. Optical signal $s_p(t)$ (p = 1, 2,…, N) is launched into the port of the space encoder, in which it is split equally into N components and constant phase shifts are inserted for these components according to the code. Then, the N components combined at the output port q are coupled into a core q of the MCF with N cores and propagate along the fibre with intercore CT. Here, we suppose that all cores with the same material and structure have a common initial length L, and the relative difference $\delta_q(t)$ are generated. This condition specifies that the propagation constants are almost the same and that power coupling between the cores is frequent. Every optical signal output from the core is launched into the decoder acting as an inverse transform of the encoder, and then finally reaches the

Tsubokawa, M.
Analysis of Multicore Fibre Transmission with Space Coding Scheme.
DOI: 10.5220/0005718301020106
In *Proceedings of the 4th International Conference on Photonics, Optics and Laser Technology (PHOTOPTICS 2016)*, pages 104-108
ISBN: 978-989-758-174-8

photodetector (PD). We can estimate the output signal

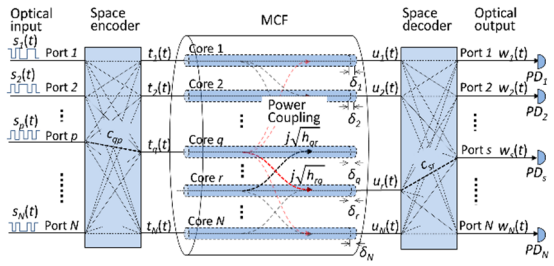

Figure 1: Block diagram of SDM transmission with a single-mode MCF based on the space-coding scheme.

$w_s(t)$ at the decoder port s in terms of matrix multiplication given by $\mathbf{W} = {}^t\mathbf{C}\cdot\mathbf{D}\cdot\mathbf{H}\cdot\mathbf{C}\cdot\mathbf{S}$, where $\mathbf{S}$ and $\mathbf{W}$ are N vectors describing input and output light signals, respectively, whereas $\mathbf{C}$, $\mathbf{H}$, and $\mathbf{D}$ are the matrices for coding, amplitude coupling, and fibre transmission, respectively. Note that ${}^t\mathbf{C}$ is the transpose of $\mathbf{C}$. The representation with the matrix elements is written as Eq. (1). Here, C_{qp} (C_{rs}) is the matrix element of $\mathbf{C}$, where the subscripts indicate the input port p (r) and output port q (s) of the encoder (decoder). For simplicity, the $s_p(t)$ polarization state is assumed to be constant throughout the entire process. In our model, $\mathbf{H}$ is approximated by the matrix of an $N \times N$ directional coupler composed of 2×2 elements. Here, h_{rq} indicates the total power transfer ratio from core q to core r in the MCF. This indicates coherent couplings on the way along a fiber when all β_r are equal. For comparison, as described later, we consider the model for matrix $\mathbf{H}$ where power coupling is repeated several times along the fibre. Assuming a lossless system, $\mathbf{H}$ is given by a unitary matrix with $h_{rq} = h_{qr}$ and $\sum_{q=1}^{N} h_{rq} = 1$ for $q, r = 1, 2,\ldots, N$. As mentioned above, the relative variation of $\delta_q(t)$ is assumed to be quite less and slow compared to the symbol lengths and rates of transmission signals $s_p(t)$ because environmental changes such as temperature affect all cores equally. Therefore, we focus on the slowly-varying phase drift difference $\beta\delta_q(t)$ rather than the length variation, which is also considered as the mean phase variation for coherently coupled components into core q. Based on Eq. (1), the output signal at the decoder's port s is written as

$$\begin{aligned} w_s(t) \propto\ & \textstyle\sum_{r=1}^{N}\{\sqrt{h_{rr}}c_{rs}c_{r1}+j\sum_{q\neq r}^{N}\sqrt{h_{rq}}c_{rs}c_{q1}\} \\ & e^{j\beta\delta_r(t)}s_1(t) + \cdots + \textstyle\sum_{r=1}^{N}\{\sqrt{h_{rr}}c_{rs}c_{rp} + \\ & j\textstyle\sum_{q\neq r}^{N}\sqrt{h_{rq}}c_{rs}c_{qp}\}e^{j\beta\delta_r(t)}s_p(t) + \cdots + \\ & \textstyle\sum_{r=1}^{N}\{\sqrt{h_{rr}}c_{rs}c_{rN}+j\sum_{q\neq r}^{N}\sqrt{h_{rq}}c_{rs}c_{qN}\} \\ & e^{j\beta\delta_r(t)}s_N(t). \end{aligned} \quad (2)$$

Because $w_s(t)$ contains all input signal components from $s_1(t)$ to $s_N(t)$, the components not involving the desired signal must be eliminated using optical code division multiplexing. In our calculation, the well-known *Hadamard* matrix is used as $\mathbf{C}$, where the polarity is realized using a phase shift of π. For ideal conditions in the absence of the optical phase drift and CT, the separate detection of the desired signal is achieved simply because ${}^t\mathbf{C}\cdot\mathbf{C} = n\mathbf{I}$ (n: integer, $\mathbf{I}$: identity matrix). In the general case of interest to us, $h_{rq} \neq 0$; however, noise components remain in the decoder outputs because of the intercore CT. In the following sections, we discuss the effectiveness of our space coding technique for MCFs with strong and weak power couplings.

$$\begin{pmatrix} w_1(t) \\ \vdots \\ w_s(t) \\ \vdots \\ w_N(t) \end{pmatrix} = \frac{1}{N}\begin{pmatrix} c_{11} & \cdots & \cdots & c_{r1} & \cdots & c_{N1} \\ \vdots & \ddots & & \vdots & & \vdots \\ c_{1s} & \cdots & c_{ss} & c_{rs} & \cdots & c_{Ns} \\ \vdots & & & c_{rr} & & \vdots \\ \vdots & & & \vdots & \ddots & \vdots \\ c_{1N} & \cdots & \cdots & c_{rN} & \cdots & c_{NN} \end{pmatrix}\begin{pmatrix} e^{j\beta_1(L+\delta_1(t))} & \cdots & \cdots & 0 & \cdots & 0 \\ \vdots & \ddots & & \vdots & & \vdots \\ \vdots & & \ddots & \vdots & & \vdots \\ 0 & \cdots & \cdots & e^{j\beta_r(L+\delta_r(t))} & \cdots & 0 \\ \vdots & & & \vdots & \ddots & \vdots \\ 0 & \cdots & \cdots & 0 & \cdots & e^{j\beta_N(L+\delta_N(t))} \end{pmatrix} \quad (1)$$

$$\times\begin{pmatrix} \sqrt{h_{11}} & \cdots & j\sqrt{h_{1q}} & \cdots & \cdots & j\sqrt{h_{1N}} \\ \vdots & \ddots & \vdots & & & \vdots \\ \vdots & & \sqrt{h_{qq}} & & & \vdots \\ j\sqrt{h_{r1}} & \cdots & j\sqrt{h_{rq}} & \sqrt{h_{rr}} & \cdots & j\sqrt{h_{rN}} \\ \vdots & & \vdots & & \ddots & \vdots \\ j\sqrt{h_{N1}} & \cdots & j\sqrt{h_{Nq}} & \cdots & \cdots & \sqrt{h_{NN}} \end{pmatrix}\begin{pmatrix} c_{11} & \cdots & \cdots & c_{1p} & \cdots & c_{1N} \\ \vdots & \ddots & & \vdots & & \vdots \\ c_{q1} & \cdots & c_{qq} & c_{qp} & \cdots & c_{qN} \\ \vdots & & & c_{pp} & & \vdots \\ \vdots & & & \vdots & \ddots & \vdots \\ c_{N1} & \cdots & \cdots & c_{Np} & \cdots & c_{NN} \end{pmatrix}\begin{pmatrix} s_1(t) \\ \vdots \\ s_p(t) \\ \vdots \\ s_N(t) \end{pmatrix}.$$

3 PERFORMANCE ANALYSIS AND RESULTS

3.1 Coding in Use of a MCF with Strong Coupling

Figure 2 shows rough sketches of (a) 4-core and (b) 8-core optical fibres. All cores in each fibre are identical. These two examples are typical of different MCF types with (a) strongly coupled cores of $h_{rq} \approx 1/N$ for $q, r = 1, 2, \ldots, N$, and (b) low crosstalk between only the nearest neighbour cores, i.e. h_{qq}, $h_{q\pm1,q} \neq 0$ and $h_{rq} \approx 0$. We first discuss the coding effect in the MCFs of the former type. Substituting $h_{rq} = 1/N$ into Eq. (2), the output signal $w_s(t)$ is approximated by

$$w_s(t) \propto \sum_{r=1}^{N}\{c_{rs}c_{r1}+j\sum_{q\neq r}^{N}c_{rs}c_{q1}\}e^{j\beta\delta_r(t)}s_1(t) + \cdots + \sum_{r=1}^{N}\{c_{rs}c_{rp}+j\sum_{q\neq r}^{N}c_{rs}c_{qp}\} e^{j\beta\delta_r(t)}s_p(t) + \cdots + \sum_{r=1}^{N}\{c_{rs}c_{rN} +j\sum_{q\neq r}^{N}c_{rs}c_{qN}\}e^{j\beta\delta_r(t)}s_N(t). \quad (3)$$

where $\sum_{q\neq r}^{N}$ indicates a sum of $N-1$ terms over all q except for $q = r$. In the case of the desired signal of $s_s(t)$ at $p = s$ in Eq. (3), we consider the amplitude coefficient of the desired signal $s_s(t)$, which is $\sum_{r=1}^{N}\{c_{rs}c_{rs} + j\sum_{q\neq r}^{N}c_{rs}c_{qs}\}e^{j\beta\delta_r(t)}$, and the other terms including other signal amplitudes, $\sum_{p\neq s}^{N}\sum_{r=1}^{N}\{c_{rs}c_{rp}+j\sum_{q\neq r}^{N}c_{rs}c_{qp}\}e^{j\beta\delta_r(t)}$. Assuming the variation of the phase drift $\beta\delta_r(t)$ is random and small, the former terms contain non-zero values of ~N and almost zero values because of the sum of squares of the matrix elements and the sum of products of the elements in different rows, respectively. The latter terms act as noise and consist of the two sums of products of matrix elements of different lines and rows, with different lines and identical rows; moreover, they are approximately zero because of the orthogonality. Consequently, we can expect that the amplitude of the desired signal will be higher than that of the noise components. However, owing to the orthogonality of coding matrices, faulty cancellation occurs when the phase drift cannot be ignored. To estimate the impact on the separate detection of the desired signal because of the phase drift, we next analyse the PD output given by,

$$|w_s(t)|^2 \propto |K_1(t)s_1(t) + \cdots + K_s(t)s_s(t) + \cdots + K_N(t)s_N(t)|^2 = \sum_{m=1}^{N}|K_m(t)|^2|s_m(t)|^2 + \sum_{m=1}^{N}\sum_{n=1}^{N}K_m(t)K_n^*(t)s_m(t)s_n^*(t), \quad (4)$$

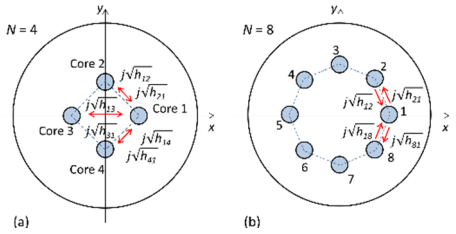

Figure 2: Two different single-mode MCFs with (a) high and equal CT between every core, and (b) low CT between only nearest neighbor cores.

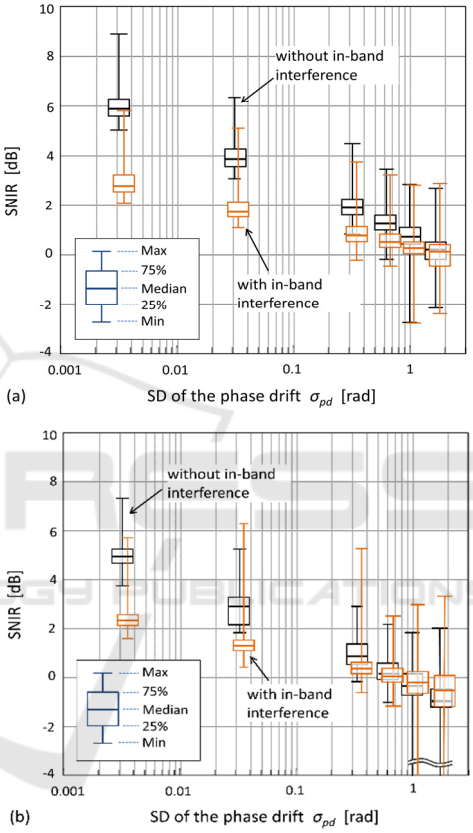

Figure 3: SNIR as a function of σ_{pd} when the desired signals (a) $s_1(t)$ and (b) $s_2(t)$ are obtained through 4-core fibre with $h_{qr} = 0.5$ ($q, r = 1, 2, \ldots, 4$). The sample number is 1000 and the box areas indicate the range within 25% above or below the median. To ensure visibility of two overlapped bars, orange-coloured bars are shifted slightly along x-axes.

where $K_m(t)$ is the amplitude coefficient of each signal $s_m(t)$ described above. Assuming that every signal exhibits the same uniform averaged power, we define the signal to interference-and-noise ratio (SNIR) simply as the intensity ratio of $|K_s(t)|^2 / (\sum_{m=1}^{N}\sum_{n=1}^{N}K_m(t)K_n^*(t) - |K_s(t)|^2)$ for the desired signal $s_s(t)$. Here, the SNIR is composed of the mutual access interference (MAI) and non-desired signal components and does not include the noise

because of the PD. If the optical carriers of each signal are fully separate, in-band interferences because of $s_m(t)s_n^*(t)$ can be neglected.

To analyse the SNIR, we assume that the phase drift difference $\beta\delta_m(t)$ follows the zero-mean normal distribution with the standard deviation (SD) σ_{pd}, because $\beta\delta_m(t)$ is mainly caused by environmental changes around a certain mean value, and it is also interpreted as the random phase difference of the lights with many intercore couplings along a fibre. Figures 3(a) and 3(b) show box plots of the SNIR as a function of σ_{pd} when the desired signals $s_1(t)$ and $s_2(t)$ are included within $w_1(t)$ and $w_2(t)$, respectively, and $N = 4$ and $h_{rq} = 0.5$ for $r, q = 1, 2, 3, 4$. The sample size is 1000 and box areas indicate the range within 25% above or below the median. Examination of Fig. 3(a) shows that the SNIR declines linearly with increasing σ_{pd}, but remains at more than 0 dB for $\sigma_{pd} < \pi/5$ in the case of no in-band interference. When the in-band interference, i.e. MAI, is added, the SNIR exhibits a remarkable degradation in the region of lower σ_{pd}. This is because of the large values of the interference components that behave as a cosine curve within small phase differences. Fig. 3(b) presents the data for the desired signal $s_2(t)$; while these show a similar trend for SNIR values: the SNIR values are lower than those in Fig. 3(a) by 0.5–1 dB because of the characteristics of the coding matrix. Summarising the results, a SNIR of more than 0 dB can be expected for the 4-core fibre when the phase drift is suppressed to within the $\sigma_{pd} \leq \pi/10$ range. However, for practical transmission, it may be necessary to reduce or compensate the phase drift because of the characteristics of the coding matrix. Summarising the results, a SNIR of more than 0 dB can be expected for the 4-core fibre when the phase drift is suppressed to within the $\sigma_{pd} \leq \pi/10$ range. However, for practical transmission, it may be necessary to reduce or compensate the phase drift because of the widely distributed SNIR values.

Furthermore, for the sake of comparison, we estimate the SNIR for a fibre model in which the matrices **D** and **H** consist of multiple matrices, i.e. $\mathbf{D}\cdot\mathbf{H} = \prod_{i=1}^{M}(\mathbf{D}_i\cdot\mathbf{H}_i)$ where M is the number of intercore couplings. According to the additivity of variance of the normal dispersion, the SD of the phase drift at each coupling is set to be $\sigma_{pd}\sqrt{M}$. Figure 4 shows the SNIR for the desired signal $s_1(t)$ as a function of σ_{pd} in the 4-core fibre with $M = 10$.

Although the SNIR rises slightly over the entire range of σ_{pd}, there is no significant difference in the results presented in Fig. 3(a).

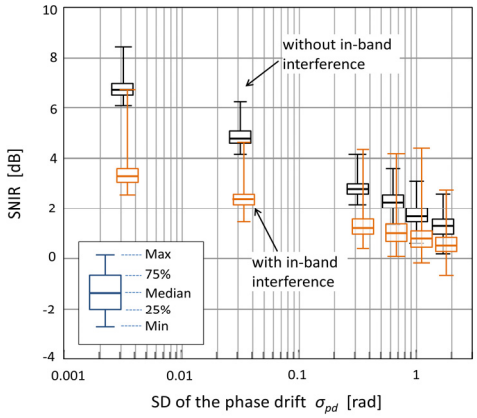

Figure 4: SNIR as a function of σ_{pd} when the desired signal $s_1(t)$ is obtained through a 4-core fibre model with multiple connections of $M = 10$.

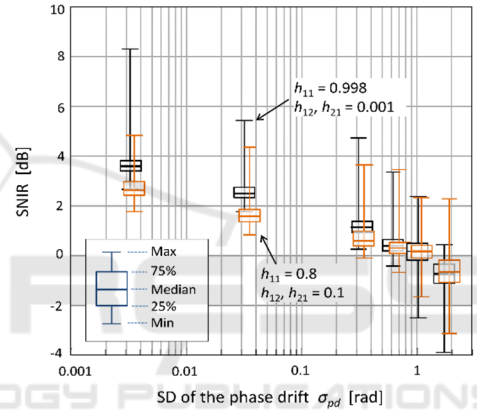

Figure 5: SNIR with in-band interferences as a function of σ_{pd} when the desired signal $s_1(t)$ is obtained through the 8-core fibre with two different CT.

3.2 Coding in Use of a MCF with Weak Coupling

Next, we analyse the coding performance for an MCF with low CT illustrated in Fig. 2(b). For simplicity, we assume that the CT takes a non-zero value only between adjacent cores, i.e. $h_{qr} = 0$ except for $r = q \pm 1$. The elements of matrix **H** are given by

$$\begin{pmatrix} \sqrt{h_{11}} & j\sqrt{h_{12}} & \cdots & 0 & \cdots & 0 & j\sqrt{h_{1N}} \\ j\sqrt{h_{21}} & \sqrt{h_{22}} & \ddots & 0 & \cdots & \vdots & 0 \\ 0 & j\sqrt{h_{32}} & \ddots & j\sqrt{h_{q-1,q}} & \cdots & 0 & \vdots \\ 0 & 0 & \ddots & \sqrt{h_{qq}} & \ddots & 0 & 0 \\ \vdots & 0 & \cdots & j\sqrt{h_{q+1,q}} & \ddots & j\sqrt{h_{N-2,N-1}} & 0 \\ 0 & \vdots & \cdots & 0 & \ddots & \sqrt{h_{N-1,N-1}} & j\sqrt{h_{N-1,N}} \\ j\sqrt{h_{N1}} & 0 & \cdots & 0 & \cdots & j\sqrt{h_{N,N-1}} & \sqrt{h_{NN}} \end{pmatrix}. \quad (5)$$

The output signal $w_s(t)$ is then written as

$$
\begin{aligned}
w_s(t) \propto\ & \sum_{q=1}^{N}\Big\{\sqrt{h_{qq}}c_{qs}c_{q1}\mathrm{e}^{j\beta\delta_r(t)} \\
& + \\
& \sum_{k=\pm1} j\sqrt{h_{q+k,q}}c_{q+k,s}c_{q1}\,\mathrm{e}^{j\beta\delta_{q+k}(t)}\Big\}s_1(t)+\cdots \\
& +\sum_{q=1}^{N}\Big\{\sqrt{h_{qq}}c_{qs}c_{qs}\mathrm{e}^{j\beta\delta_q(t)} \\
& + \\
& \sum_{k=\pm1} j\sqrt{h_{q+k,q}}c_{q+k,s}c_{qs}\,\mathrm{e}^{j\beta\delta_{q+k}(t)}\Big\}s_s(t)+\cdots \\
& +\sum_{q=1}^{N}\Big\{\sqrt{h_{qq}}c_{qs}c_{qN}\mathrm{e}^{j\beta\delta_q(t)} \\
& + \\
& \sum_{k=\pm1} j\sqrt{h_{q+k,q}}c_{q+k,s}c_{qN}\,\mathrm{e}^{j\beta\delta_{q+k}(t)}\Big\}s_N(t).
\end{aligned}
\tag{6}
$$

Assuming that $\beta\delta_r(t)$ is negligible between the nearest neighbour cores, the amplitude of the desired signal $w_s(t)$ is given by $\sum_{q=1}^{N}\Big\{\sqrt{h_{qq}}c_{qs}c_{qs}\mathrm{e}^{j\beta\delta_q(t)} + \sum_{k=\pm1} j\sqrt{h_{q+k,q}}c_{q+k,s}c_{qs}\,\mathrm{e}^{j\beta\delta_{q+k}(t)}\Big\}$. The maximum value of the first term is $N\sqrt{h_{qq}}$, and the second term approaches zero because of the orthogonality of matrix **C**. Moreover, for the other signal components, the coefficient $\sum_{m\neq s}\sum_{q=1}^{N}\Big\{\sqrt{h_{qq}}c_{qs}c_{qm}\mathrm{e}^{j\beta\delta_q(t)} + \sum_{k=\pm1} j\sqrt{h_{q+k,q}}c_{q+k,s}c_{qm}\,\mathrm{e}^{j\beta\delta_{q+k}(t)}\Big\}$ approaches zero. Consequently, we can expect the separate detection of the desired signal for a small phase drift. For this type of MCF, we can expect a better coding gain because the number of cores, i.e. code length, and coupling pairs that act as noise sources are correspondingly higher and lower than those for the MCF with strong coupling discussed above. Using Eqs. (4) and (6), the SNIR is calculated for the case of the 8-core optical fibre model. Figure 5 shows the SNIR as a function of σ_{pd} when the power transfer ratios are (a) $h_{12} = 0.1$ and $h_{11} = 0.8$, and (b) $h_{12} = 0.001$ and $h_{11} = 0.998$, equivalent to the extinction ratios of −6 and −17 dB, respectively. It is clear that the SNIR declines with increasing σ_{pd}, and remains positive in the $\sigma_{pd} \leq \pi/10$ range. The SNIR is improved by ~1 dB in the case of smaller h_{12}, but this case is considered to be fairly insensitive to CT. Furthermore, compared to the results in Fig. 5 and Fig. 3(a), we can observe a slight improvement of ~1 dB for the SNIR values shown in Fig. 5. The improvement is lesser than expected, because the fault cancellations for many undesired signal components are caused by the phase drifts and these weaken the coding gain.

4 CONCLUSIONS

We have analysed the space coding characterization in MCF transmission with strong and weak intercore couplings. Separate detection for the desired signal can be achieved without optical MIMO processing with an SNIR of more than 0 dB, achieved when the phase drift of the optical signal in each core is suppressed, typically to within ~π/10. In future studies, we will perform simulation experiments in an in-depth investigation and evaluate bit error rate characteristics as well as identify a procedure for control of the phase drifts in MCF transmission.

REFERENCES

Arik, S. Ö., Askarov, D., Kahn, J. M., 2013. 'Effect of mode coupling on signal processing complexity in mode-division multiplexing,' *J. Lightw. Technol.*, vol. 31, pp. 423–431.

Kitayama, K., Wang, X., Wada, N., 2006. 'OCDMA over WDM PON–Solution path to gigabit-symmetric FTTH,' *J. Lightw. Technol*, vol. 24, pp. 1654–1662.

Hayashi, T., Taru, T., Shimakawa, O., Sasaki, T., Sasaoka, E., 2011. 'Design and fabrication of ultra-low crosstalk and low-loss multi-core fiber,' *Opt. Exp*., vol. 19, pp. 16576–16592.

Hernandez, V. J., Mendez, A. J., Bennett, C. V., Lennon, W. J., 2005. 'Simple robust receiver structure for gigabit Ethernet O-CDMA using matrix codes,' *J. Lightw. Technol.*, vol. 23, pp. 3105–3110.

Mendez, A. J., Gagliardi, R. M., Hernandez, V. J., Bennett, C. V., Lennon, W. J., 2003. 'Design and performance analysis of wavelength/time (W/T) matrix codes for optical CDMA,' *J. Lightw. Technol*., vol. 21, pp. 2524–2533.

Ryf, R., Essiambre, R. –J., Randel, S., Gnauck, A. H., Winzer, P. J., Hayashi, T., Sasaki, T., 2011. 'MIMO-based crosstalk suppression in spatially multiplexed 56-Gb/s PDM-QPSK signals in strongly-coupled 3-core fibre,' *IEEE Photon. Technol. Lett*., vol. 23, pp. 1469-1471.

Sakaguchi, J., Puttnam, B. J., Klaus, W., Awaji, Y., Wada, N., Kanno, A., Kawanishi, T., Imamura, K., Inaba, H., Mukasa, K., Sugizaki, R., Kobayashi, T., Watanabe, M., 2013. '305 Tb/s space division multiplexed transmission using homogeneous 19-core fibre,' *J. Lightw. Technol.,* vol. 31, pp. 554-562.

Sakamoto, T., Mori, T., Wada, M., Yamamoto, T., Yamamoto, F., 2015. 'Coupled multicore fiber design with low intercore differential mode delay for high-density space division multiplexing,' *J. Lightw. Technol.*, vol. 33, pp. 1175–1181.

Shah, A. R., Hsu, R. C. J., Tarighat, A., Sayed, A. H., Jalali, B., 2005. 'Coherent optical MIMO (COMIMO),' *J. Lightw. Technol.*, vol. 23, pp. 2410–2419.

Winzer, P. J., Gnauck, A. H., Konczykowska, A., Jorge, F., Dupuy, J.-Y., 2011. 'Penalties from in-band crosstalk for advanced optical modulation format,' *Proc. ECOC,* 2011, Tu.5.B.7.

Xia, C., Amezcua-Correa, R., Antonio-Lopez, N. B. E., Arrioja, D. M., Schulzgen, A., Richardson, M., Liñares, J., Monteo, E., Zhou, X., Li, G., 2012. 'Hole-assisted few mode multicore fiber for high-density space-division multiplexing,' *IEEE Photon. Technol. Lett.*, vol. 24, pp. 1914–1917.